Sun *et al.*
European Journal of Medical Research (2025) 30:365
https://doi.org/10.1186/s40001-025-02630-3

European Journal of Medical Research

RESEARCH Open Access

Aminooxyacetic acid ameliorates alcohol-induced learning and memory deficits through BDNF-TrkB pathway and calcium homeostasis

Zhen Sun[1†], Meinan Nie[1†], Xunling Wang[1†], Bolin Jiao[1], Jiayi Fu[1] and Ailin Du[1*]

Abstract

Chronic alcohol-related brain damage (ARBD) is mainly manifested as learning and memory impairment and cognitive decline in the long term. Ca^{2+} plays a key role in learning and memory impairment. The increase of intracellular Ca^{2+} concentration can directly cause mitochondrial dysfunction, destroy normal physiological signal transduction, and accelerate the process of learning and memory decline. Aminooxyacetic acid (AOAA), a selective inhibitor of Cystathionineβ-synthase (CBS), has a good effect on a variety of diseases, including improving stroke and reducing the incidence of convulsions. However, its potential in maintaining learning and memory functions by regulating Ca^{2+} and mitochondrial functional status remains uncertain. In this study, chronic alcoholism rats and human neuroblastoma cells (SHSY-5Y) were used as the research objects to establish a chronic alcohol-related brain damage model. We aimed to elucidate the specific mechanisms by which AOAA protects learning and memory functions in alcohol-induced learning and memory impairment. Through Morris water maze test, LTP test, Western blot (WB), immunohistochemistry (IHC), mitochondrial observation under electron microscope, calcium ion concentration measurement and mitochondrial membrane potential measurement, it was found that AOAA could not only regulate the level of endoplasmic reticulum stress (ERS) caused by H_2S elevation, but also maintain the role of valve of Sec61 channel on Ca^{2+} by restoring the level of BIP, a key indicator of ERS, significantly alleviate mitochondrial dysfunction caused by Ca^{2+} overload, and optimize learning and memory function. The mechanism may be closely related to the BDNF-TrkB pathway.

Keywords Chronic alcoholism, H_2S, BDNF-TrkB pathway, CBS, BIP, Learning and memory, Mitochondrial damage, Endoplasmic reticulum stress, AOAA

Introduction

Alcohol abuse and chronic alcoholism have become global public health crises. According to the World Health Organization (WHO) Global Status Report on Alcohol and Health 2018, approximately 3 million people die each year due to alcohol-related causes, accounting for 5.3% of the total global mortality. Alcohol consumption notably raises the risk of liver disease, heart conditions, mental health disorders, and several cancers, while also placing a heavy burden on society and families. As a

†Zhen Sun, Meinan Nie and Xunling Wang contributed equally to this research and are co-first authors.

*Correspondence:
Ailin Du
duailin@126.com
[1] Sino-UK International Joint Laboratory of Brain Injury in Henan Province, Henan International Joint Laboratory of Neuromodulation, Department of Physiology and Pathophysiology, School of Basic Medical Sciences, Xinxiang Medical University, No. 601, Jinsui Road, Xinxiang, China

neurotoxic substance, chronic alcohol exposure leads to structural and functional alterations in the brain, which subsequently impair learning and memory functions. Studies have shown that chronic alcohol use may induce neuronal apoptosis in key regions of the brain, such as the hippocampus, which is closely related to the decline in cognitive abilities, including learning and memory[1].

In recent years, the pathological mechanisms underlying chronic alcoholism have become a focal point of research. As a neuromodulator, hydrogen sulfide (H_2S) maintains normal cognitive function by promoting BDNF and NMDA receptor activity and energy metabolism[2]. It is cytoprotective at lower than physiological concentrations (nM level), but long-term exposure to lower doses slightly above physiological levels (e.g., 1.02 ppm) can induce apoptosis through the mitochondrial toxicity pathway [3–5]. Notably, the role of H_2S in chronic alcoholism has gained increasing attention. H_2S is an endogenous gaseous signaling molecule produced by cystathionine β-synthase (CBS) [6]. Studies have indicated that chronic alcohol consumption can enhance CBS activity in the brain, leading to abnormal elevations in H_2S levels, which in turn contribute to neuronal damage [7]. Furthermore, H_2S activates the BDNF-TrkB signaling pathway, influencing endoplasmic reticulum stress (ERS) and disrupting intracellular Ca^{2+} homeostasis, ultimately affecting mitochondrial function and promoting neuronal apoptosis [8].

The BDNF-TrkB signaling pathway plays a critical role in the development, survival, and functional regulation of the nervous system. Brain-derived neurotrophic factor (BDNF) is a key member of the neurotrophic factor family. By binding to the TrkB receptor (Tropomyosin-Related Kinase B), BDNF induces receptor dimerization and autophosphorylation, triggering downstream signaling cascades, including the activation of RAS (rat sarcoma protein) and the phosphatidylinositol 3-kinase (PI3K) signaling pathway, which mediate neuroprotection [9]. In chronic alcoholism, aberrant activation of the BDNF-TrkB pathway is closely associated with ERS, exacerbating neuronal damage. BDNF, through the BDNF/TrkB and downstream phosphoinositide-specific phospholipase Cγ (PLCγ)—inositol 1,4,5-trisphosphate (IP3) and PI3K pathways, induces mitochondrial fission, affects mitochondrial length in neuronal dendrites, and alters the distribution of mitochondria to postsynaptic sites [10, 11]. Therefore, exploring potential strategies to regulate chronic alcohol-induced effects is of paramount importance.

The Sec61 channel is a transmembrane protein complex located on the endoplasmic reticulum (ER) membrane, primarily composed of three different subunits: Sec61α, Sec61β, and Sec61γ, forming a heterotrimer [12]. It forms a hydrophobic channel within the body [12, 13]. The Sec61 channel is a transmembrane protein complex located on the ER membrane, mainly composed of three different subunits, including Sec61α, which forms a compact helical bundle consisting of 10 transmembrane (TM) helices, thereby creating an opening for the transmembrane channel. This pore can open laterally to the lipid bilayer through a lateral gate formed by a pair of TM helices, TM2 and TM7. In addition, the pore also exhibits a ring made of six hydrophobic amino acid residues and an α-helical plug portion that is located inside the lumen of the pore to block the channel [14]. Sec61 functions as the primary channel for precursor polypeptides to enter the ER membrane or lumen. In eukaryotes, most secretory proteins and membrane proteins are targeted to the ER via their N-terminal signal sequences, and it also provides a channel for Ca^{2+} to move from the ER lumen to the cytosol [15–18]. The open Sec61 channel facilitates the release of calcium ions from the ER into the cytoplasm, playing an important role during Ca^{2+} dysregulation.

Research has confirmed that heavy-chain binding protein (BIP) is one of the most important molecular chaperones in the ER. Its expression increases during ER stress and is considered one of the key markers of ERS [19]. It can limit ER Ca^{2+} leakage. When the expression of BIP decreases, Ca^{2+} is uncontrollably leaked through the Sec61 protein complex, and this leakage severely disrupts the ER membrane's ability to maintain high cytosolic Ca^{2+} concentrations [20–22]. The chaperone protein BIP on the ER binds to the Sec61 complex, localized in the ER lumen at the tyrosine 344 site of Sec61α's seventh ring, limiting the flow of Ca^{2+} from the ER lumen to the cytosol [23].

Aminooxyacetic acid (AOAA), a potent CBS inhibitor, has been widely used in biological research. Studies have shown that AOAA specifically inhibits CBS activity, thereby reducing its ability to catalyze the conversion of homocysteine to H_2S and lowering tissue H_2S levels. This effect has been shown to improve cognitive function in rats with chronic alcoholism [24]. Additionally, AOAA can block the BDNF-TrkB signaling pathway, restore ERS levels, and alleviate mitochondrial damage.

In this study, we used the Morris water maze and LTP tests to assess learning and memory in rats, combined with qPCR, WB, and immunohistochemistry to analyze the expression of relevant molecules. Electron microscopy was used to examine mitochondrial morphology, and JC-1 mitochondrial membrane potential assays were employed to evaluate mitochondrial function. This research sought to investigate the role of H_2S in learning and memory impairments in rats with chronic alcoholism and its effect on ERS via the BDNF-TrkB pathway.

Through these comprehensive analyses, we hope to reveal the mechanisms by which H_2S contributes to cognitive dysfunction in chronic alcoholism and to identify potential therapeutic targets for alcohol-induced neurodegeneration. The following section provides a detailed examination of AOAA's effects at the genetic level and the underlying mechanisms involved.

Materials and methods

Animal model

Eighty SD rats [25] (180–220 g) were randomly divided into four groups: control group (Con), AOAA intervention group (Con + AOAA), chronic alcoholism model group (Model), and chronic alcoholism + AOAA treatment group (Model + AOAA), with 20 rats in each group. Except for the control and AOAA intervention groups, the rats in the model and chronic alcoholism + AOAA treatment groups were given a 6% alcohol solution for 28 days to establish the chronic alcoholism model. After day 14, the rats in the AOAA intervention and chronic alcoholism + AOAA treatment groups were intraperitoneally injected with AOAA at a dose of 5 mg/kg [26], while the control and model groups were injected with an equal amount of saline for 14 days.

After the water maze test, 12 SD rats were randomly selected from the original control group and the original chronic alcoholism group for subsequent experiments. The original control group was divided into a control group and a K252a-negative control group, with 6 rats in each group. And the original chronic alcoholism group was divided into a chronic alcoholism group and a K252a-inhibition group, with 6 rats in each group. K252a was dissolved in sterile artificial cerebrospinal fluid (ACSF)/dimethyl sulfoxide (DMSO; 1:1, v/v) (Sigma-Aldrich). Subsequently, we used K252a for intracerebroventricular injection (icv) to rats, and the specific interventions were as follows:

(1) Control group: daily saline (i.p.) and ACSF/DMSO (icv) for 9 days;
(2) K252a negative control group: after 14 days, daily saline (i.p.) and K252a (icv) for 9 days;
(3) Chronic alcoholism model group: daily 6% alcohol solution (i.p.) and ACSF/DMSO (icv) for 9 days;
(4) K252a inhibition group: daily 6% alcohol solution (i.p.) and K252a (icv) for 9 days.

Cell culture

SH-SY5Y cells were cultured in DMEM high-glucose medium (containing 10% fetal bovine serum, 100 U/ml penicillin, and 100 mg/ml streptomycin), with the medium being changed every 48 h. The cells were then seeded at a density of 1×10^5/ml into 96-well plates, with five replicate wells per group. When the cell density reached about 70%, the model group and AOAA treatment group were exposed to ethanol at a concentration of 400 mmol/L, while the control and AOAA negative control groups received an equal volume of medium. After continuing culture for 12 h, the AOAA treatment and AOAA negative control groups were given AOAA at a concentration of 0.5 mmol/L. After another 12 h of incubation, 10 μL of MTT was added to each well. After 4 h of incubation, the culture medium was discarded. Then, 100 μL of DMSO was added to each well, and the plate was shaken at low speed for 10 min. Absorbance at 570 nm was measured using a microplate reader. SH-SY5Y cells were seeded in 24-well plates at a density of 1×10^5/ml. When the cell density reached 70%–80%, ethanol was added at final concentrations of 50, 100, 200, 400, and 800 mmol/L, and continued culture was carried out for 24 h. After washing with PBS and fixing with 4% paraformaldehyde, cells were stained with Hoechst 33342 (5 μg/mL) at room temperature for 30 min. Fluorescence microscopy was used to observe and photograph the stained cells, and apoptotic cells were counted in five high-power fields (×400) for each group. The apoptotic rate (%) was calculated as (number of apoptotic cells/total cell number) × 100%.

Stereotaxic surgery and intracerebroventricular injection

The rats were anesthetized with 3% sodium pentobarbital (0.2 mL/100 g, i.p.) and placed in a stereotaxic apparatus for surgery. The skin over the skull was removed to expose the junction of the sagittal and coronal sutures. A small hole (2 mm in diameter) was drilled on the right hemisphere skull, the bone was thinned, and the dura mater was exposed at the following coordinates: AP, − 1.0 mm; ML, − 1.5 mm; DV, − 3.0 mm. A stainless steel tube (approximately 0.9 mm in diameter, 20 mm in length) was inserted into the right lateral ventricle, and a soft core was rapidly inserted to prevent cerebrospinal fluid leakage. The stainless steel screw was fixed with dental cement. To ensure the drug was properly delivered, the injection needle was slowly pulled out halfway, and the needle was left in place for 2 min before being completely withdrawn.

Electron microscopy

Hippocampal tissue was removed from − 80 °C storage, cut into 1 mm^3 blocks, and fixed in 4% glutaraldehyde within 1 min. After washing with PBS, the tissue was fixed in 1% osmium tetroxide. The tissue was dehydrated in graded acetone, embedded in epoxy resin, and sectioned into ultrathin slices. The slices were stained

with lead citrate and uranyl acetate and observed under a transmission electron microscope.

Mitochondrial Ca^{2+} ATPase activity assay

Following the ATPase activity assay kit instructions, tissue samples were homogenized in an ice-water bath, centrifuged at 2500×*g* for 10 min. The supernatant was used for enzyme reaction, followed by centrifugation at 3500×*g* for 10 min, and phosphate was measured in the supernatant. Absorbance was measured at 636 nm, and ATPase activity was calculated using the following formula:

ATPase activity (U/mg prot) = (Measured OD − Control OD)/(Standard OD − Blank OD) × Standard concentration (0.02 μmol/mL) × 6 × 7.8/Sample protein concentration (mg/mL).

Western blotting

Total proteins were extracted from tissues and cells, and protein concentration was determined using the BCA protein assay kit (Beyotime Biotechnology, Shanghai, China). The proteins were separated by SDS-PAGE (10% SDS-PAGE) and transferred to PVDF membranes, which were then blocked for 2 h at 37 °C with serum. The membranes were incubated overnight at 4 °C with primary antibodies (CBS 1:1000, BDNF 1:1000, TrkB 1:1500, BIP 1:1500, β-actin 1:10,000), followed by incubation with corresponding secondary antibodies for 1 h at 37 °C. Protein bands were visualized using an ECL kit (NCM, Suzhou, China) and analyzed with a ChemiDoc imaging system (Bio-Rad, Hercules, USA). β-actin was used as a loading control.

H_2S content measurement

Four rats from each group were randomly selected, anesthetized intraperitoneally, and decapitated. The hippocampal tissue was promptly dissected and stored in liquid nitrogen. Absorbance was measured at 670 nm using the H_2S detection kit (Mlbio, Shanghai, China). The H_2S content in the hippocampus was measured as the amount of H_2S per unit weight of tissue (nmol/g).

Morris water maze learning and memory assessment

On day 28 following model induction, 8 rats from each group were randomly selected for the navigation and spatial probe tests. The first four days were dedicated to positioning navigation tests. Each day, the starting quadrant was changed in a counterclockwise direction, and each rat was trained four times per day. A camera recorded the swimming path of each rat, and data were analyzed using EthoVision XT 8 behavior recording software (Noldus). After locating the submerged platform, each rat was allowed to stay on it for 30 s to consolidate its memory. The maximum training time was 60 s. If a rat did not find the submerged platform within 60 s, it was guided to the platform and allowed to remain there for 30 s. In the navigation test, the latency and swimming distance to the platform were recorded. After the navigation test, the platform was removed, and the spatial probe test was conducted to assess the rat's memory of the platform's location. The rats were released from the quadrant opposite the target quadrant, and their swimming time was recorded for 180 s, with the number of times they crossed the platform's location counted. (After the water maze test, 12 SD rats were randomly selected from the original control group and the original chronic alcoholism group for subsequent K252a experiments.)

Interface-type thermostatic bath perfusion system

Lens Cleaning Tissue filter paper was placed flat in the groove of the interface-type thermostatic bath to drain artificial cerebrospinal fluid (ACSF). The peristaltic pump was activated, initially washing with 30 mL of ultra-pure water, then 30 mL of ACSF, and then closing the perfusion system to begin circulating ACSF. The flow rate of the peristaltic pump was adjusted to 4–5 mL/min. The ACSF was heated to 30–32 °C by a TC324B temperature control device before entering the bath. A glass slide was placed over the groove to prevent gas diffusion, and all equipment was grounded to eliminate 50 Hz noise interference.

Brain slice preparation

SD rats were euthanized by intraperitoneal injection of 3% sodium pentobarbital (0.2 mL/100 g). A 25 mL syringe was used to withdraw pre-chilled perfusion solution into the left ventricle while simultaneously cutting the right atrium for heart perfusion. The skull, meninges, and brain tissue were carefully separated, exposing the brain. The brainstem, olfactory bulb, and cerebellum were removed to avoid damaging the hippocampus. The brain tissue was carefully placed into the LEICA VT 1000S vibratome's groove with cutting solution, and 350 μm thick slices were prepared, with 4–5 hippocampal slices collected.

Long-term potentiation (LTP) learning and memory evaluation

Glass electrodes (outer diameter 1.2 mm, inner diameter 0.69 mm) were prepared using a P-97 puller for recording. The temperature-controlled interface bath was incubated for 1 h, and brain slices were transferred to the recording chamber. The stimulation electrode was placed in the hippocampus CA3 radiate layer, and the recording electrode was positioned in the CA1 region. After setting, stimulation-response curves were constructed using

half the maximum stimulus intensity, followed by high-frequency stimulation (HFS) to induce LTP. Biological signals were amplified, and noise at 50 Hz was removed. The digital signals were analyzed using Spike2 software.

Immunohistochemistry

Paraffin sections of hippocampal tissue were deparaffinized, followed by antigen retrieval in citrate buffer. Sections were incubated with 3% hydrogen peroxide (Beyotime, Shanghai, China), sealed with 5% bovine albumin (BSA) for 30 min, and then incubated with primary antibodies overnight at 4 °C. After incubation with HRP-conjugated secondary antibodies, diaminobenzidine.

(DAB) was added, and the sections were counterstained with hematoxylin. Stained sections were photographed and analyzed using Image Pro Plus 6.0 software.

Fluorescent quantitative PCR

CBS, BDNF, TrkB, and BIP primers, along with the Transcriptor First Strand cDNA Synthesis Kit (HiScript III All-in-one RT SuperMix Perfect for qRT-PCR, Vazyme), were utilized to synthesize cDNA from mRNA. RNAse inhibitors were employed to prevent degradation. Amplification was carried out using Taq Pro Universal SYBR qRT-PCR Master Mix (Vazyme). The mRNA expression levels were normalized to glyceraldehyde-3-phosphate dehydrogenase (GAPDH) expression. The primer sequences of the target genes are shown in Table 1.

Mitochondrial membrane potential

SH-SY5Y cells were seeded in 6-well black plates at a density of 1×10^6 cells/well. Prior to the experiment, 1 ml JC-1 staining solution was added to each well according to the JC-1 kit instructions and incubated for 20 min. After washing, centrifuging, and resuspending, the mitochondrial membrane potential was observed and photographed using a laser confocal microscope. The depolarization of the mitochondria was typically measured based on the ratio of red and green fluorescence.

Fluorescence method for measuring intracellular Ca^{2+}

The Fluo 3-AM calcium ion fluorescence probe was utilized to measure intracellular Ca^{2+}concentrations. A xenon lamp (SUTTER Lambda DG-4) with a sampling rate of 1 Hz was used to collect the signal at 488 nm. SH-SY5Y cells were seeded on coverslips coated with 100 μg/mL poly-L-lysine (diameter = 30 mm) and cultured for 24 h. After 48 h, the calcium fluorescence dye Fluo 3-AM (5 μM, Dojindo, Japan) was loaded in Krebs-HEPES buffer at room temperature for 30 min. The buffer consisted of (mM): 135 NaCl, 6 KCl, 2 $CaCl_2$, 1.2 $MgCl_2$, 10 D-glucose, and 10 HEPES (pH 7.4). After washing the coverslips three times, the cells were de-esterified in Krebs-HEPES buffer without indicators for at least 20 min before imaging. The coverslips were then placed in a perfusion chamber, and fluorescence signals were recorded in real-time using a microscope with a xenon lamp (488 nm filter) and a Zeiss Axio Observer A1 microscope (40×, 1.3 NA objective). Two-thirds of the cell body was designated as the region of interest (ROI) for image analysis. The calcium signal (F) was recorded in real-time. The signal was normalized by dividing by the baseline signal (F_0), expressed as F/F_0. To measure $[Ca^{2+}]_i$, a high-calcium solution (5 mM Ca^{2+}) and a Ca^{2+}/EGTA-free solution were perfused. The fluorescence was measured as Fmax and Fmin. The formula for measuring $[Ca^{2+}]_i$ is:

$$F\left[Ca^{2+}\right]_i = [(F - Fmin) / (Fmax - F)] \times Kd, (Kd = 400\,nm)$$

Mitochondrial ATPase activity measurement

ATPase decomposes adenosine triphosphate (ATP) to produce adenosine diphosphate (ADP) and inorganic phosphate. The amount of inorganic phosphate released indicates the level of ATPase activity. Following the instructions of the ultramicro total ATPase assay kit, an appropriate amount of tissue was homogenized in an ice-water bath and then centrifuged at 2500×*g* for 10 min. After the enzyme reaction in the supernatant, the sample was centrifuged at 3500×*g* for 10 min. The resulting supernatant was used to measure phosphate concentration. Absorbance was measured at 636 nm, and ATPase activity was calculated using the following formula:

ATPase activity (U/mg prot) = (Measured OD − Control OD)/(Standard OD − Blank OD) × Standard concentration (0.02 μmol/mL) × 6 × 7.8/Sample protein concentration (mg/mL).

Immunoprecipitation

Cells were lysed using Triton X-100 buffer and incubated with the relevant primary antibodies overnight at 4 ℃. After treatment with the proteasome inhibitor MG132 (Univ, Shanghai, China), the lysates were mixed with Protein G Plus/Protein A-Agarose beads (Abxin,

Table 1 Primer design

Gene	Forward primer	Reverse primer
BIP	TTCCGAGGAACACTGTGGTG	GTCAGGGGTCGTTCACCTTC
CBS	CAGTTCAAGCCGATCCACCT	ACGCCATTGTTGCGGTATTG
BDNF	TTTGGGGCAGACGAGAAAGC	ACCTGGTGGAACTCAGGGT
TrkB	GTCAGCCCTCACGTCACTTC	CAACTGCGGTAGCAGGACA

Shanghai, China) and incubated for 2 h at 4 ℃. The beads were washed three times with lysis buffer, and the sample was heated for 10 min in 5× sample loading buffer. Both the protein samples and immunoprecipitates were analyzed through Western blotting.

Statistical analysis

Data are presented as mean ± SEM. Statistical analysis was carried out using GraphPad Prism 9.5. Comparisons between two groups were made using the *t*-test, while comparisons among multiple groups were conducted using one-way analysis of variance (ANOVA), with a significance level set at $\alpha = 0.05$. A *p*-value of < 0.05 was considered statistically significant. Detailed consumables are listed in Supplementary Table 1 and Supplementary Table 2.

Results

AOAA intervention restores learning and memory impairments induced by chronic alcoholism

After the chronic alcoholism model was established (Fig. 1a), the morris water maze and LTP experiments were conducted. No significant differences were found between the groups regarding swimming speed and total movement distance (Fig. 1b; $P > 0.05$). However, in terms of platform latency and platform dwell time (Fig. 1b), the Model group exhibited significantly prolonged latency and reduced platform dwell time compared to the Con group ($P < 0.05$). In contrast, the Model + AOAA group showed significant cognitive recovery, with shorter platform latency and longer dwell time ($P < 0.01$).

Figure 1c illustrates the swimming trajectories in the morris water maze test, where the Model group's trajectories were more scattered, indicating impaired spatial learning and memory. In contrast, the Model + AOAA group showed more concentrated trajectories, indicating cognitive improvement. These results further support the recovery of cognitive function in the Model + AOAA group. The escape latency over time is shown in Fig. 1d. Over the course of the training days, all groups exhibited a general decline in escape latency. The Model group consistently had higher escape latency than the Con and Con + AOAA groups, while the Model + AOAA group showed lower escape latency compared to the Model group. Moreover, following high-frequency stimulation, synaptic transmission efficiency in the Model group was not significantly enhanced, indicating impaired LTP (Fig. 1e). In the Model + AOAA group, LTP was partially restored, with a significantly higher post-stimulation PSP slope 20 min after stimulation compared to the Model group. These findings suggest that AOAA can alleviate alcohol-induced LTP impairments.

AOAA downregulates CBS and inhibits the BDNF/TrkB pathway

Immunohistochemical results showed that, compared to the Con group, the protein expression of CBS, BDNF, and TrkB was significantly increased in the Model group ($P < 0.01$). In the Model + AOAA group, the expression levels of CBS, BDNF, and TrkB were significantly decreased ($P < 0.05$), but still higher than those in the control group. In contrast, the protein expression of BIP was significantly decreased in the Model group ($P < 0.001$). After AOAA treatment, BIP expression was upregulated again ($P < 0.001$), but still lower than in the control group (Fig. 2a, b). Similarly, Western blot and qPCR results also confirmed that AOAA treatment could reverse the upregulation of CBS, BDNF, and TrkB, and the downregulation of BIP caused by chronic alcoholism. Western blot results (Fig. 2c, d) further showed that the protein levels of CBS, BDNF, TrkB, and BIP were significantly elevated or reduced in the Model group, while in the Model + AOAA group, these protein levels were partially restored but still significantly lower than in the control group. Additionally, qPCR analysis (Fig. 2e) showed that chronic alcohol exposure led to significant changes in the mRNA expression of CBS, BDNF, TrkB, and BIP, which were reversed by AOAA treatment. Specifically, in the Model group, the mRNA expression of CBS, BDNF, and TrkB was significantly increased ($P < 0.001$), while BIP mRNA expression was significantly decreased ($P < 0.001$). After AOAA treatment, the mRNA levels of CBS, BDNF, and TrkB were significantly decreased ($P < 0.001$), and the expression of BIP mRNA was significantly higher than that in the model group ($P < 0.001$).

For further exploration of the intracellular pathways, co-immunoprecipitation assays was conducted to demonstrate the endogenous interaction between BIP and Sec61α proteins in SH-SY5Y (Fig. 2f, $p < 0.05$). This suggests that AOAA improves alcohol-induced cellular stress responses by influencing the interaction between BIP and Sec61α. Finally, hydrogen sulfide (H_2S) measurements (Fig. 2g) showed that the H_2S content in the Model group rats was significantly increased ($P < 0.05$), while in the Model + AOAA group, H_2S content was significantly decreased ($P < 0.01$), further proving the reparative effect of AOAA on the physiological changes related to chronic alcoholism.

AOAA modulates endoplasmic reticulum stress via the BDNF/TrkB pathway

Figure 3a illustrates the experimental timeline and treatment protocol. Seven-week-old male SD rats were acclimated to the environment and then treated with either a 6% ethanol solution or drinking water. On day 28, they received either saline or K252a injections, with

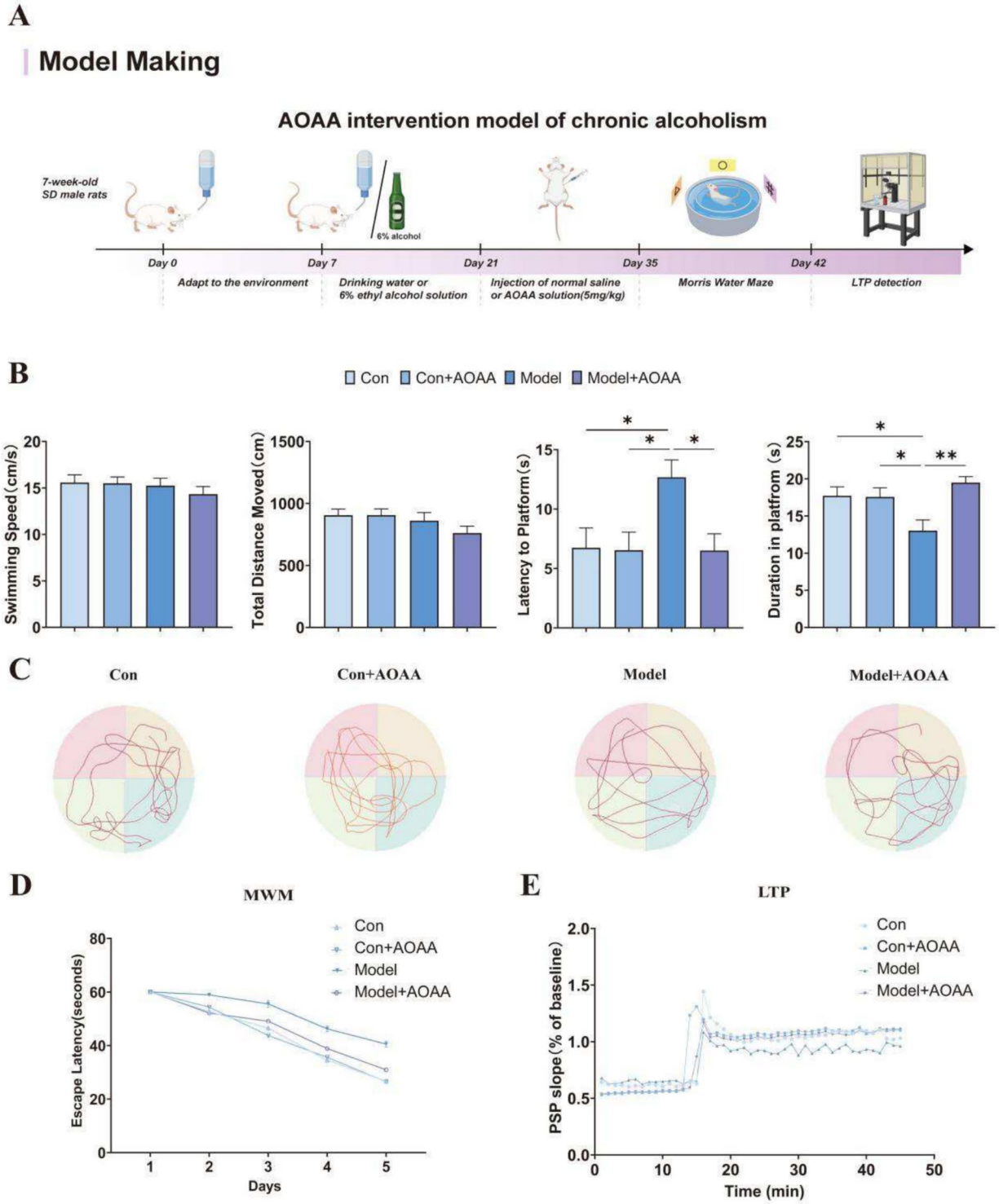

Fig. 1 AOAA intervention restores learning and memory impairments induced by chronic alcoholism. **a** Schematic of the rat model. **b** Bar graph showing swimming speed, total movement distance, platform latency, and platform dwell time in the morris water maze test. **c** Trajectory plots of each group in the morris water maze test. **d** Line graph showing the changes in escape latency for each group. **e** LTP experiment assessing synaptic plasticity in each group. *(Con: Control group; Model: Chronic alcoholism model group; Con + AOAA: AOAA negative control group; Model + AOAA: Chronic alcoholism model + AOAA treatment group; $^{*}P < 0.05$, $^{*}P < 0.01$)

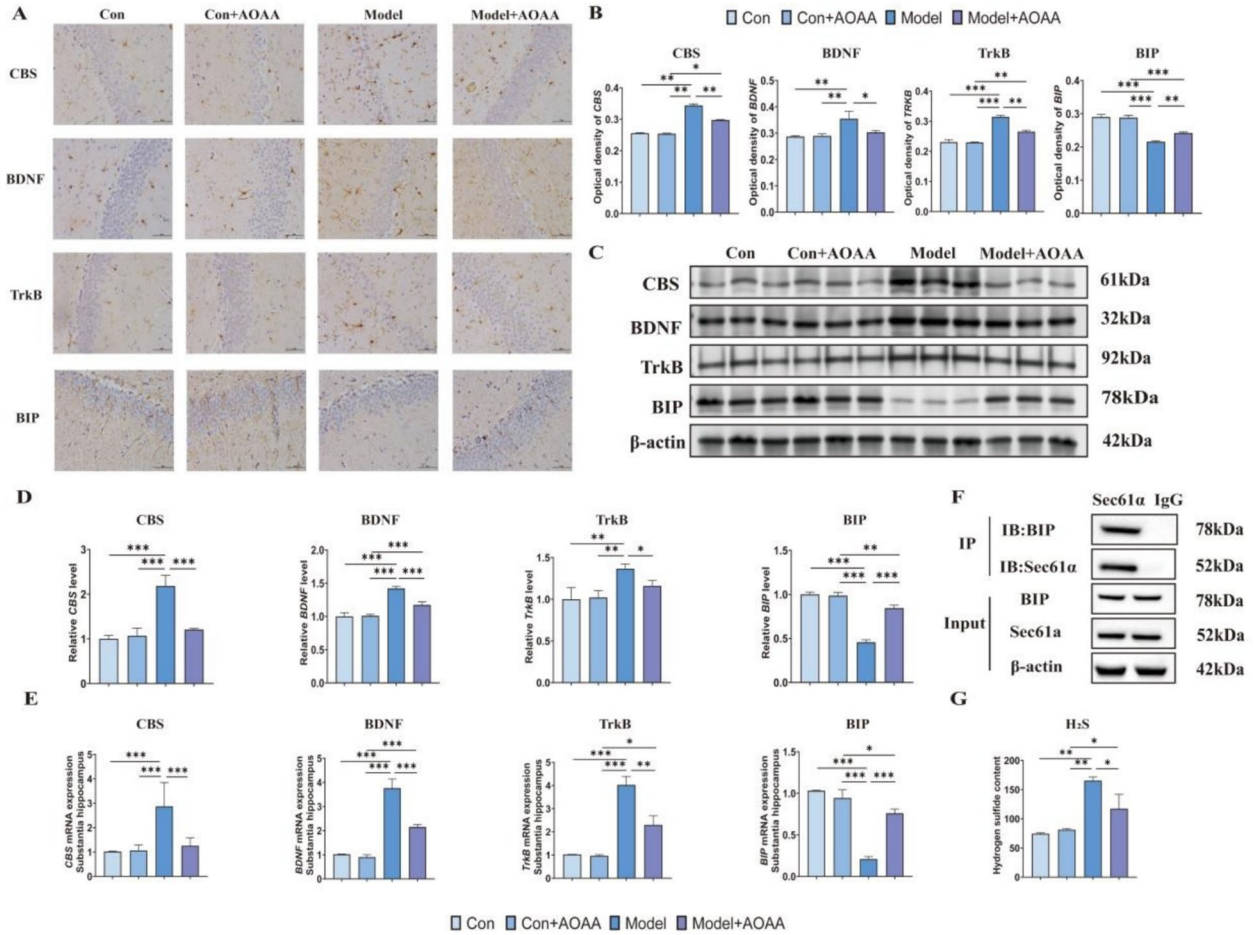

Fig. 2 AOAA downregulates CBS and inhibits the BDNF/TrkB pathway. **a** Representative immunohistochemistry images of each group (n = 3) Scale bar = 50 μm. **b** Histogram showing the optical density of immunohistochemical results. **c** Western blot analysis of CBS, BDNF, TrkB, and BIP protein levels in each group. **d** Quantitative analysis of WB results. **e** qPCR detection of CBS, BDNF, TrkB, and BIP mRNA expression levels in each group. **f** Immunoprecipitation Experiment: binding of Sec61α to BIP in Different Groups. **g** Quantitative analysis of hippocampal H_2S content in each group. *(Con: Control group; Model: Chronic alcoholism model group; Con + AOAA: AOAA negative control group; Model + AOAA: Chronic alcoholism model + AOAA treatment group; *$P < 0.05$, **$P < 0.01$, **$P < 0.001$)

LTP assessment conducted on day 37. Immunohistochemical staining showed that, compared to the Con group, the protein expression levels of TrkB and BDNF were significantly upregulated in the Model group (Model), whereas they were significantly downregulated in the K252a intervention group. As expected, BIP showed the opposite expression trend in the above experiments (Fig. 3b, c). Western blot (WB) and qPCR results demonstrated that K252a was able to inhibit the downregulation of BIP and the upregulation of TrkB induced by chronic alcoholism (Fig. 3d–f). LTP experimental results (Fig. 3g) indicated that rats in the Model group displayed significant deficits in LTP responses, while the Model + K252a group, treated with K252a, showed a recovery in LTP responses. This confirms the importance of the BDNF/TrkB pathway in chronic alcoholism and the restorative effects of K252a on LTP. These results further suggest that K252a alleviates alcohol-induced neuronal damage by inhibiting the BDNF/TrkB pathway.

AOAA affects calcium influx, mitochondrial damage, and ATPase activity

We further assessed the impact of AOAA on intracellular calcium ion concentration using immunofluorescence. The results showed that the calcium ion concentration in the Model group was significantly higher than that in the Con and Con + AOAA groups ($P < 0.01$). After AOAA treatment, the intracellular calcium ion concentration significantly decreased, indicating that AOAA could alleviate alcohol-induced calcium ion influx (Fig. 4a, d). Subsequently, we evaluated changes in mitochondrial membrane potential (ΔΨm). In the Model group, the red particles (representing regions with high

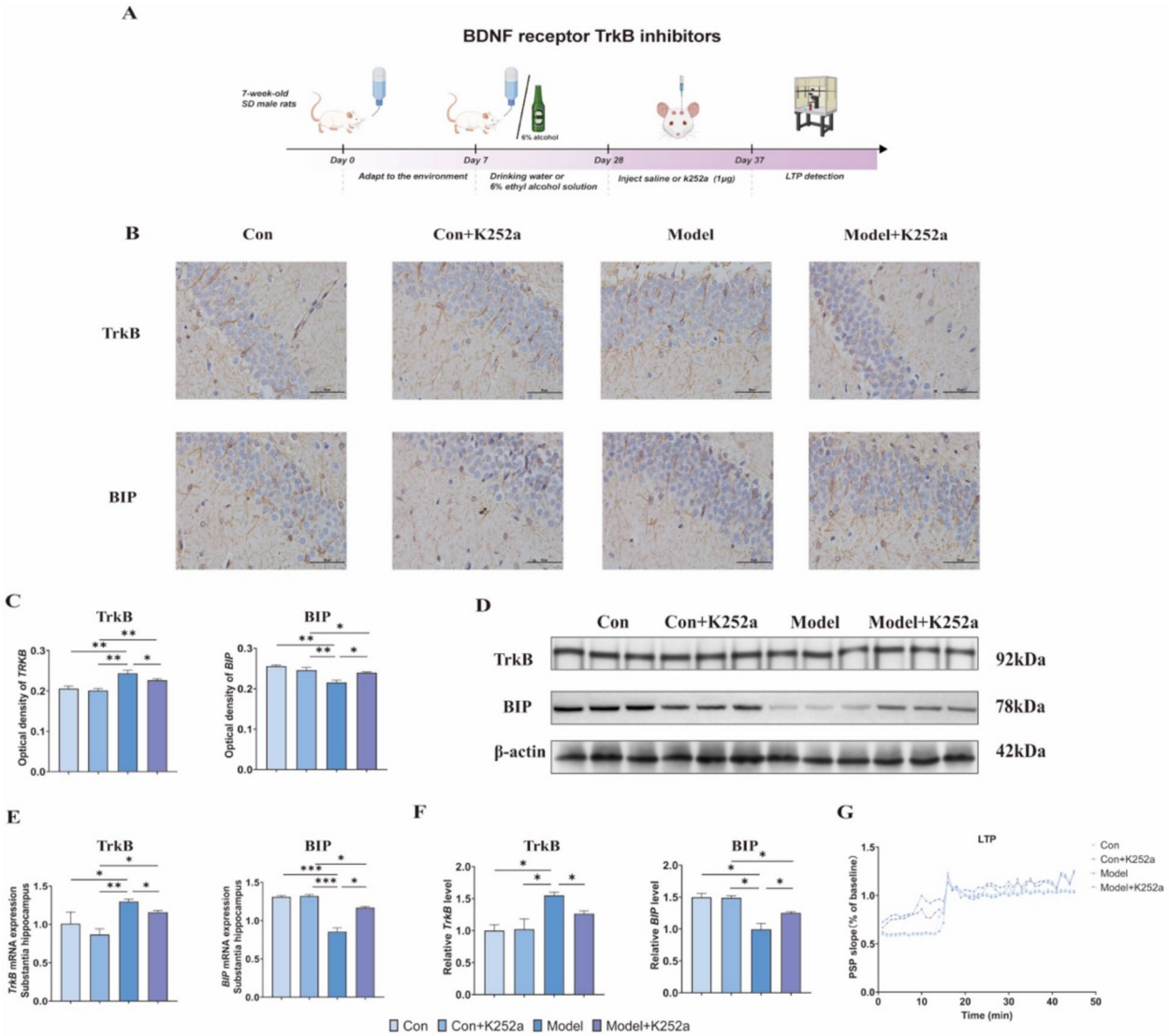

Fig. 3 AOAA Modulates Endoplasmic Reticulum Stress via the BDNF/TrkB Pathway. **a** Schematic of the rat model. **b** Immunohistochemical staining of TrkB and BIP protein expression in each group (Scale bar = 50 μm). **c** Histogram showing the optical density of immunohistochemistry results. **d** Western blot analysis of TrkB and BIP protein expression levels in each group (n = 3).**e, f** Quantitative analysis of the Western blot results for TrkB and BIP protein expression in each group. **g** LTP experiment assessing synaptic plasticity in each group. *(Con: Control group; Model: Chronic alcoholism model group; Con + K252a: K252a negative control group; Model + K252a: Chronic a alcoholism model + K252a treatment group; *$P < 0.05$, *$P < 0.01$)

mitochondrial membrane potential) from JC-1 staining significantly decreased, while the green particles (representing regions with low membrane potential) significantly increased, indicating that alcohol exposure caused a loss of mitochondrial membrane potential. In contrast, in the Model + AOAA group, the red particles from JC-1 staining significantly increased, and the green particles decreased, suggesting that AOAA treatment effectively restored the mitochondrial membrane potential damage caused by alcohol (Fig. 4b, e). Next, transmission electron microscopy was used to observe the mitochondria in each group (Fig. 4c). The results showed that in the Model group, mitochondria exhibited significant swelling and inner membrane damage (indicated by red arrows), indicating alcohol-induced mitochondrial damage in hippocampal neurons. However, these damage changes were improved in the Model + AOAA group, with no significant swelling or damage observed. Furthermore, ATPase activity assays showed that compared to the control group, ATPase activity was significantly reduced in

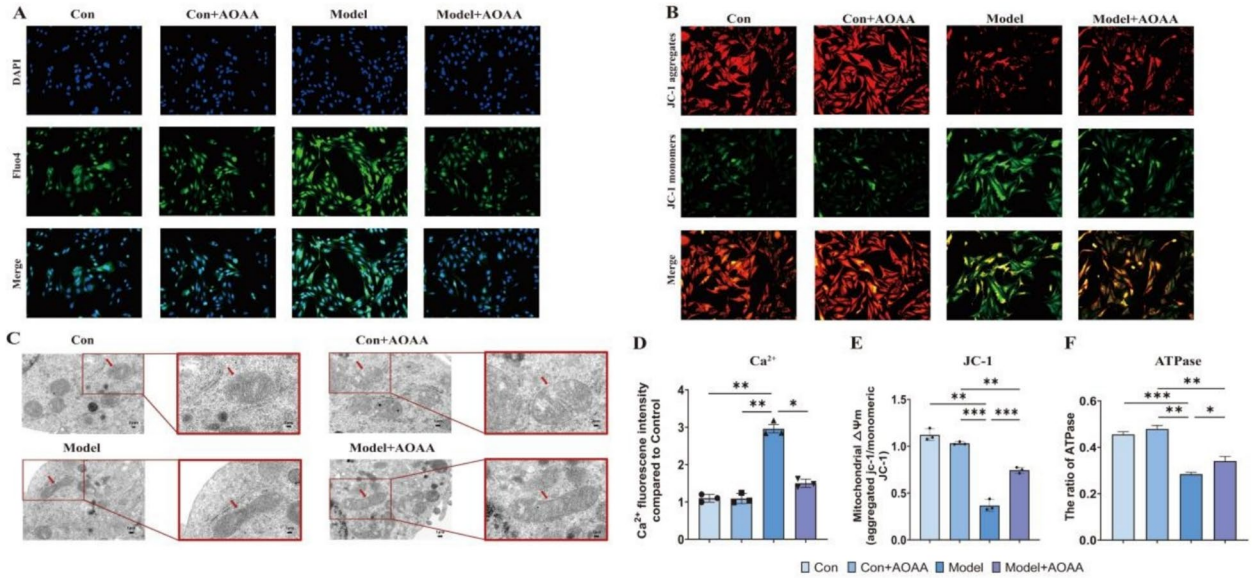

Fig. 4 AOAA Affects Calcium Influx, Mitochondrial Damage, and ATPase Activity. **a, d** Quantitative detection of intracellular calcium levels in neuronal cells using a kit (green: mitochondria; red: mitochondrial calcium uniporter (MCU)). **b, e** JC-1 staining to detect changes in mitochondrial membrane potential. (n = 3, Scale bar = 50 μm. **c** TEM observation of mitochondrial morphological changes in neurons across different groups (n = 3). **f** Results of ATPase activity. *(Con: Control group; Model: Chronic alcoholism model group; Con + AOAA: AOAA negative control group; Model + AOAA: Chronic alcoholism model + AOAA treatment group; *$P < 0.05$, **$P < 0.01$, **$P < 0.001$)

the Model group ($P < 0.001$), while in the Model + AOAA group, ATPase activity was partially restored ($P < 0.05$). This further supports the role of AOAA in restoring the abnormal cellular energy metabolism induced by alcohol.

Dynamic regulation of downstream BDNF-TrKB pathway by H_2S

According to the above research results, we initially mapped the mechanism diagram of H_2S regulation of downstream BIP protein and Sec61 channel through BDNF-TrkB pathway. After chronic alcoholism, the massive activation of CBS promoted the expression of hydrogen sulfide, which interfered with the level of ER stress by activating the BDNF-TrkB pathway. BIP, a key indicator of ERS, was further inhibited in this link. After BIP downregulation, the openness of the sec61 channel increases, and a large amount of Ca^{2+} flows from the endoplasmic reticulum to the cytoplasm through the Sec61 channel, thus causing nerve cell injury (Fig. 5).

Discussion

Alcohol abuse and chronic alcoholism are global public health issues that severely impact individual health, family well-being, and social stability. Alcohol not only significantly increases the risk of liver diseases, cardiovascular diseases, mental health issues, and cancers, but it also imposes a tremendous burden on society and families. Previous research has demonstrated that chronic alcoholism results in impairments in learning, memory, cognitive function, and psychological behavior [27]. Furthermore, chronic alcoholism affects the function of the nervous system through various mechanisms, with hydrogen sulfide (H_2S) metabolic dysregulation being a key factor.

H_2S is recognized as the third gas signaling molecule in the body, following carbon monoxide (CO) and nitric oxide (NO) [28]. Previous studies have established that, at physiological concentrations, H_2S exerts a range of biological effects, including vasodilation, enhanced microcirculation, antioxidant activity, anti-inflammatory properties, and the preservation of learning, memory, and cognitive function in rats [29]. In the brain, H_2S is mainly produced through the metabolism of sulfur-containing amino acids (e.g., methionine converting to cysteine), a process catalyzed by enzymes such as cystathionine β-synthase (CBS). CBS is an enzyme found in the mammalian brain that depends on pyridoxal-5'-phosphate (vitamin B6). Under specific conditions, CBS catalyzes the reaction between L-homocysteine and L-cysteine, leading to the production of hydrogen sulfide (H_2S). As a result, elevated CBS expression enhances H_2S production [30].

Previous research has indicated that TRPA1 is widely expressed in neurons and serves as an oxidative stress sensor that triggers calcium signaling cascades under pathological conditions such as H_2S exposure [3, 31],

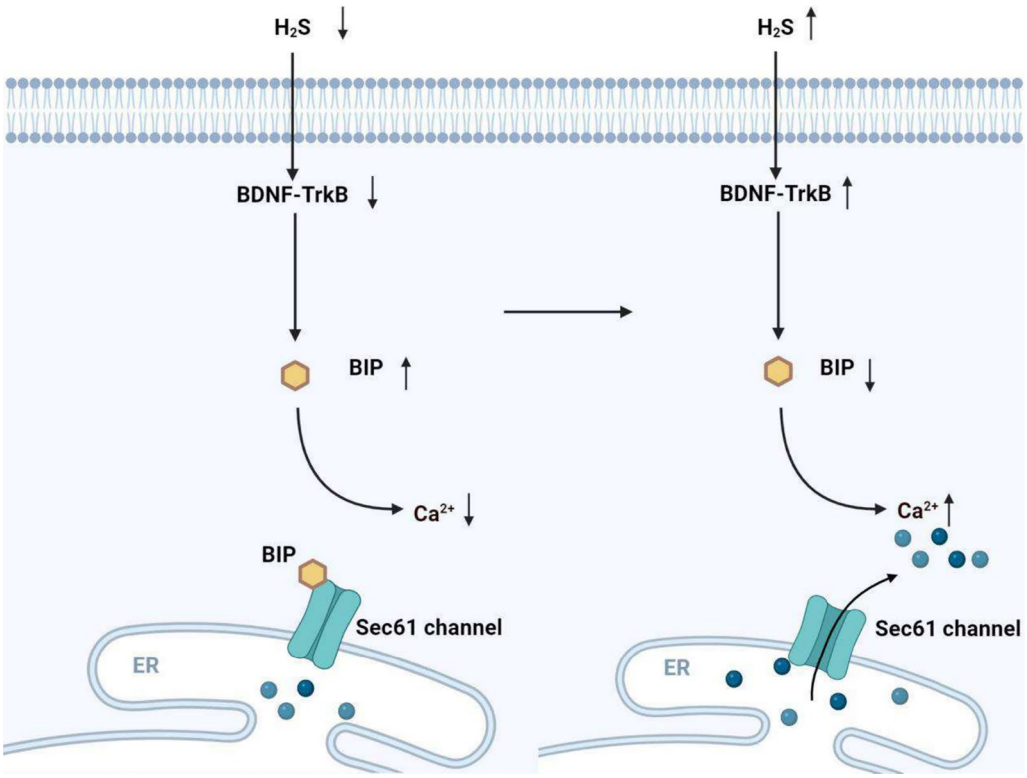

Fig. 5 Diagram of downstream mechanism of H_2S (Changes in gas, pathway and protein expression are indicated by ↑and ↓)

and elevated H_2S levels can be harmful to the brain. This toxicity is mainly mediated through the TRPA1 receptor, causing an overload of intracellular calcium [32]. The excess calcium disrupts cellular homeostasis, resulting in mitochondrial swelling, reduced ATPase activity, and disturbances in energy metabolism. ATPase is an important membrane protein complex located in the mitochondrial inner membrane and performs multiple key functions. Mitochondria play a crucial role in regulating apoptosis, generating free radicals, maintaining calcium and ATP levels, and protecting cells and tissues. As a result, mitochondrial dysfunction can impact various cellular and systemic functions [33, 34]. Studies have shown that increased intracellular H_2S levels facilitate Ca^{2+} influx, causing mitochondrial damage and impairing ATPase activity [26]. Similar phenomena were observed in this study. In chronic alcohol exposure, CBS expression is upregulated, leading to excess H_2S production. Further, transmission electron microscopy results confirmed that mitochondrial swelling and damage were observed in the chronic alcoholism group.

To reverse the upregulation of CBS induced by alcohol, we used AOAA to intervene in the chronic alcoholism model animals. AOAA is a well-established CBS inhibitor. Previous studies have demonstrated that it decreases CBS activity by inhibiting its conversion of homocysteine to H_2S, thus reducing H_2S levels in tissues [34]. Our prior research [35] also showed that AOAA binds with CBS to form a schiff base, inhibiting its activity, thus reducing H_2S production. This further diminishes Ca^{2+} influx and mitochondrial Ca^{2+} overload, helping to alleviate mitochondrial damage induced by chronic alcoholism [36]. Moreover, by lowering endogenous H_2S production, AOAA can reduce mitochondrial damage and the decline in ATPase activity caused by chronic alcoholism.

Previous studies have suggested that hydrogen sulfide might activate the BDNF/TrkB pathway, reduce endoplasmic reticulum stress, and lead to a reduction in the expression of BIP (immunoglobulin binding protein) [37]. To further explore the mechanisms of calcium ion influx and mitochondrial damage induced by chronic alcoholism, we assessed the expression of BDNF, TrkB, and BIP using qPCR and WB. The results showed that in the chronic alcoholism group, the BDNF/TrkB pathway was activated, while BIP expression was downregulated. BIP is an important calcium-binding molecular chaperone in the endoplasmic reticulum, involved in protein folding, maintaining homeostasis, and preventing Ca^{2+} leakage from the endoplasmic reticulum. When BIP expression decreases, the Sec61 complex causes Ca^{2+} leakage and exacerbates mitochondrial calcium loading through Ca^{2+} extrusion, ultimately leading to cell

apoptosis [27]. However, after AOAA intervention, this change was reversed. To further confirm the role of the BDNF/TrkB pathway in AOAA regulation of BIP expression, we injected a TrkB inhibitor, K252a, into the hippocampus of rats. The results showed that K252a could reverse the downregulation of BIP expression induced by chronic alcoholism, confirming that AOAA regulates BIP through the BDNF-TrkB pathway.

The BDNF/TrkB pathway plays a vital role in neuronal development, differentiation, and survival, and insufficient BDNF/TrkB activity is often associated with neurodegeneration [38]. Studies have shown that, within physiological concentration ranges, H_2S can alleviate homocysteine-induced endoplasmic reticulum stress and neuronal apoptosis in rat hippocampi by upregulating the BDNF-TrkB pathway [39]. Interestingly, this study found that prolonged excessive H_2S may downregulate BIP expression via the BDNF-TrkB pathway, causing severe endoplasmic reticulum stress, mitochondrial dysfunction, and neuronal death. However, the differential effects of hydrogen sulfide at varying concentrations on the specific mechanisms still require further research.

The precise regulation of calcium concentration is essential for mitochondrial energy metabolism and cell survival, and its imbalance may lead to ATP synthesis disorders and pathological states [40]. The uptake of calcium (Ca^{2+}) from the cytosol by mitochondria through the calcium monotransporter (MCU complex) is dependent on the electrochemical gradient of the inner mitochondrial membrane [41, 42]. The increase in mitochondrial calcium concentration activates dehydrogenases of the tricarboxylic acid cycle (TCA) (e.g., pyruvate dehydrogenase, α-ketoglutarate dehydrogenase), thereby enhancing NADH production, which ultimately drives oxidative phosphorylation through F-ATP synthase (mitochondrial atpase) and enhances ATP synthesis [43–45]. However, excess mitochondrial calcium (such as calcium overload) causes mitochondrial membrane potential collapse, inhibits F-atpase activity, reduces ATP production, and may trigger the opening of the mitochondrial permeability transition pore (mPTP) to release reactive oxygen species (ROS) and cytochrome c and trigger apoptosis [46–48].

Existing alcohol use disorder (AUD) drugs, such as naltrexone and acamaminate, mainly target the opioid system or glutamatergic system, while AOAA may provide a new dimension of action by regulating hydrogen sulfide metabolism and mitochondrial function [49]. For example, CBS inhibition may alleviate alcohol-induced oxidative stress and neuroinflammation, forming a synergy with the glutamate modulatory effects of acamentous acid [50]. And there is a close connection between LTP recovery and behavioral improvement [51]. By promoting processes such as neurogenesis, repair, and synaptic plasticity, LTP recovery can enhance cognitive and motor behaviors. As a potential therapeutic drug, the effects of AOAA on LTP and the mechanisms through which LTP recovery leads to behavioral improvement still require further research. However, current studies have shown AOAA's potential in treating certain diseases.

Related studies also suggest that AOAA intervention can improve learning and memory functions as well as synaptic plasticity in chronic alcoholism rats. Of course, our study has certain limitations, there are significant interspecies differences in the H_2S metabolic pathways between rodents and humans.Besides, the study using only male rats and not exploring the effect of gender on alcohol neurotoxicity or AOAA efficacy, which may limit the generalability of the conclusions. Although the body weight range of SD rats (180–220 g) was similar, individual metabolic differences may lead to different metabolic rates of alcohol and AOAA, affecting drug effects. Balance of baseline physiological parameters (e.g., liver function) among the groups needs to be confirmed.We will focus on these issues in subsequent experiments.

In conclusion, the pathway by which AOAA improves learning and memory may involve inhibiting CBS activity, reducing H_2S generation induced by chronic alcoholism, suppressing the BDNF/TrkB pathway, and upregulating BIP expression, thereby alleviating intracellular calcium overload and mitigating mitochondrial dysfunction. Chronic alcoholism activates CBS and promotes excessive H_2S production, while AOAA, as a CBS inhibitor, reduces H_2S production and mitigates neuronal damage caused by alcoholism.

Supplementary Information

The online version contains supplementary material available at https://doi.org/10.1186/s40001-025-02630-3.

Additional file1 (DOCX 16 KB)

Additional file2 (ZIP 30555 KB)

Authors contribution

Zhen Sun, Meinan Nie and Xunling Wang contributed equally to this work as co-first authors. Zhen Sun was responsible for the conception and design of the study, data collection, and analysis.Meinan Nie contributed to the interpretation of data and wrote the manuscript. Xunling Wang contributed to the methodology and statistical analysis. Bolin Jiao and Jiayi Fu were responsible for creating the figures and analyzing the data. Ailin Du (corresponding author) supervised the entire project, provided guidance on the study design, and was involved in final manuscript approval.

Funding

The authors would like to acknowledge the financial support received for conducting the research, writing, and publishing this article. The study was funded by the Doctoral Research Initiation Project of Xinxiang Medical University (Project No. 505367) and the Henan Province Key Scientific Research Projects of Higher Education Institutions (Project No. 15A310006).

Data availability
Data is provided within the manuscript or supplementary information files.

Declarations

Ethics approval and consent to participate
This animal study was authorized by the Animal Ethics Committee of Xinxiang Medical University and was carried out in full compliance with local laws and regulations, ensuring ethical treatment of the animals throughout the research.

Competing interests
The authors declare no competing interests.

Received: 7 March 2025 Accepted: 23 April 2025
Published online: 05 May 2025

References

1. Akbar M, Baick J, Calderon F, Wen Z, Kim HY. Ethanol promotes neuronal apoptosis by inhibiting phosphatidylserine accumulation. J Neurosci Res. 2006;83(3):432–40. https://doi.org/10.1002/jnr.20744.
2. Spalloni A, de Stefano S, Gimenez J, et al. The Ying and Yang of hydrogen sulfide as a paracrine/autocrine agent in neurodegeneration: focus on amyotrophic lateral sclerosis. Cells 2023;12(13). https://doi.org/10.3390/cells12131691.
3. Liu Y, Cao Y, Li H, et al. Mitochondrial homeostatic imbalance-mediated developmental toxicity to H(2)S in embryonic zebrafish. Environ Pollut. 2025;367: 125588. https://doi.org/10.1016/j.envpol.2024.125588.
4. Rong F, Wang T, Zhou Q, et al. Intelligent polymeric hydrogen sulfide delivery systems for therapeutic applications. Bioact Mater. 2023;19:198–216. https://doi.org/10.1016/j.bioactmat.2022.03.043.
5. Zhang K, Meng J, Bao W, Liu M, Wang X, Tian Z. Mitochondrion-targeting near-infrared fluorescent probe for detecting intracellular nanomolar level hydrogen sulfide with high recognition rate. Anal Bioanal Chem. 2021;413(4):1215–24. https://doi.org/10.1007/s00216-020-03086-6.
6. Dilek N, Papapetropoulos A, Toliver-Kinsky T, Szabo C. Hydrogen sulfide: an endogenous regulator of the immune system. Pharmacol Res. 2020;161: 105119. https://doi.org/10.1016/j.phrs.2020.105119.
7. Tareen K, Clifton EG, Perumalswami P, Mellinger JL, Winder GS. Treatment of alcohol use disorder: behavioral and pharmacologic therapies. Clin Liver Dis. 2024;28(4):761–78. https://doi.org/10.1016/j.cld.2024.06.011.
8. Wei HJ, Xu JH, Li MH, et al. Hydrogen sulfide inhibits homocysteine-induced endoplasmic reticulum stress and neuronal apoptosis in rat hippocampus via upregulation of the BDNF-TrkB pathway. Acta Pharmacol Sin. 2014;35(6):707–15. https://doi.org/10.1038/aps.2013.197.
9. Minichiello L. TrkB signalling pathways in LTP and learning. Nat Rev Neurosci. 2009;10(12):850–60. https://doi.org/10.1038/nrn2738.
10. S KS, Swain M, Dagda RK. BDNF-TrkB signaling in mitochondria: implications for neurodegenerative diseases. Mol Neurobiol. 2025;62(2):1756–69 https://doi.org/10.1007/s12035-024-04357-4.
11. Chen L, Zhang Y, Wang Z, et al. Activation of GPER1 by G1 prevents PTSD-like behaviors in mice: illustrating the mechanisms from BDNF/TrkB to mitochondria and synaptic connection. CNS Neurosci Ther. 2024;30(7): e14855. https://doi.org/10.1111/cns.14855.
12. Bai-xin W, Shu-qiu W, Wen-bo Q, Shu-xiang W, Xiao-ru M, Ting Z. Effects of ganoderma lucidum spores on cytochrome c and mitochondrial calcium in the testis of NIDDM rats. Natl J Androl. 2006;12:1072–5. https://doi.org/10.13263/j.cnki.nja.2006.12.004.
13. Junxiong L, Yi W. Effects of Danshensu on myocardial fibrosis by interacting with endoplasmic reticulun Ca2+ leakage channel SEC61α in mouse heart. Hebei Med J. 2021;43(12):1844–7.
14. Witham CM, Paxman AL, Baklous L, Steuart RFL, Schulz BL, Mousley CJ. Cancer associated mutations in Sec61γ alter the permeability of the ER translocase. PLoS Genet. 2021;17(8): e1009780. https://doi.org/10.1371/journal.pgen.1009780.
15. Peng B, Yang Q, R BJ, et al. Role of alcohol drinking in Alzheimer's disease, Parkinson's disease, and amyotrophic lateral sclerosis. Int J Mol Sci 2020;21(7). https://doi.org/10.3390/ijms21072316.
16. Koob GF, Colrain IM. Alcohol use disorder and sleep disturbances: a feed-forward allostatic framework. Neuropsychopharmacology. 2020;45(1):141–65. https://doi.org/10.1038/s41386-019-0446-0.
17. Abrahao KP, Salinas AG, Lovinger DM. Alcohol and the brain: neuronal molecular targets, synapses, and circuits. Neuron. 2017;96(6):1223–38. https://doi.org/10.1016/j.neuron.2017.10.032.
18. Jun-chang L, Cui-hong Z, Fen X, Hua-ning W, Yu-ting Q. Effect of isoflurane on the cognitive function and expression of myelin basic protein (MBP) and phosphorylated neurofilament heavy polypeptide (pNF-H) in the hippocampus of middle-aged mice. Progr Mod Biomed. 2019;19(08):1425–9. https://doi.org/10.13241/j.cnki.pmb.2019.08.006.
19. Zanchao L. Bip mediates Er stress-induced tau hyperphosphorylation and the protection of Sil1 [Doctor]. 2012.
20. Daverkausen-Fischer L, Pröls F. Regulation of calcium homeostasis and flux between the endoplasmic reticulum and the cytosol. J Biol Chem. 2022;298(7): 102061. https://doi.org/10.1016/j.jbc.2022.102061.
21. Parys JB, Van Coppenolle F. Sec61 complex/translocon: The role of an atypical ER Ca(2+)-leak channel in health and disease. Front Physiol. 2022;13: 991149. https://doi.org/10.3389/fphys.2022.991149.
22. Linxweiler M, Müller CSL. Role of the SEC62 gene in dermato-oncology - impact on tumor cell biology, prognostication, and personalized therapy management. J Dtsch Dermatol Ges. 2022;20(9):1187–99. https://doi.org/10.1111/ddg.14817.
23. Schäuble N, Lang S, Jung M, et al. BiP-mediated closing of the Sec61 channel limits Ca2+ leakage from the ER. Embo j. 2012;31(15):3282–96. https://doi.org/10.1038/emboj.2012.189.
24. Yang B, Su Y, Han S, et al. Aminooxyacetic acid hemihydrochloride inhibits osteoclast differentiation and bone resorption by attenuating oxidative phosphorylation. Front Pharmacol. 2022;13: 980678. https://doi.org/10.3389/fphar.2022.980678.
25. Glover EJ, Khan F, Clayton-Stiglbauer K, Chandler LJ. Impact of sex, strain, and age on blood ethanol concentration and behavioral signs of intoxication during ethanol vapor exposure. Neuropharmacology. 2021;184: 108393. https://doi.org/10.1016/j.neuropharm.2020.108393.
26. Du A, Dai X, Dong J, et al. Effects of aminooxyacetic acid on hippocampal mitochondria in rats with chronic alcoholism: the analysis of learning and memory-related genes. J Integr Neurosci. 2019;18(4):451–62. https://doi.org/10.31083/j.jin.2019.04.1119.
27. Huerta de la Cruz S, Rodríguez-Palma EJ, Santiago-Castañeda CL, et al. Exogenous hydrogen sulfide restores CSE and CBS but no 3-MST protein expression in the hypothalamus and brainstem after severe traumatic brain injury. Metab Brain Dis. 2022;37(6):1863–74. https://doi.org/10.1007/s11011-022-01033-1.
28. Kimura H. Hydrogen sulfide (H(2)S)/Polysulfides (H(2)S(n)) signalling and TRPA1 channels modification on sulfur metabolism. Biomolecules. 2024;14(1). https://doi.org/10.3390/biom14010129.
29. Du A, Chen Y, Qiao S, et al. Analysis of microRNAs and the microRNA-messengerRNA regulatory network in chronic alcohol exposure. Front Pharmacol. 2024;15:1377501. https://doi.org/10.3389/fphar.2024.1377501.
30. Petrosino M, Zuhra K, Kopec J, Hutchin A, Szabo C, Majtan T. H(2)S biogenesis by cystathionine beta-synthase: mechanism of inhibition by aminooxyacetic acid and unexpected role of serine. Cell Mol Life Sci. 2022;79(8):438. https://doi.org/10.1007/s00018-022-04479-9.
31. Çakır M, Aydın A, Fırat S, Şekerci G, Bircan B, Öz S. Protective effect of transient receptor potential ankyrin 1 inhibition on renal ischemia reperfusion injury in rats. J Biochem Mol Toxicol. 2025;39(1): e70132. https://doi.org/10.1002/jbt.70132.
32. Bełtowski J. Synthesis, metabolism, and signaling mechanisms of hydrogen sulfide: an overview. Methods Mol Biol. 2019;2007:1–8. https://doi.org/10.1007/978-1-4939-9528-8_1.
33. Xuan D, Peng-Yan F, Jia-Bao H. Effects of aminooxyacetic acid on hippocampus mitochondria and fibrous actin in rats with chronic alcoholism. Chin J Gerontol. 2018;38(20):4996–9.
34. Vamecq J, Dessein AF, Fontaine M, et al. Mitochondrial dysfunction and lipid homeostasis. Curr Drug Metab. 2012;13(10):1388–400. https://doi.org/10.2174/138920012803762792.

35. Du AL, Qin HZ, Jiang HB, Fu PY, Lou K, Xu YM. Aminooxyacetic acid improves learning and memory in a rat model of chronic alcoholism. Neural Regen Res. 2018;13(9):1568–74. https://doi.org/10.4103/1673-5374.237120.
36. Anwar M, Amin MR, Balaji Ragunathrao VA, et al. Tyrosine phosphorylation of S1PR1 leads to chaperone BiP-mediated import to the endoplasmic reticulum. J Cell Biol. 2021;220(12). https://doi.org/10.1083/jcb.202006021.
37. He J, Chen Z, Kang X, et al. SIRT1 mediates H(2)S-ameliorated diabetes-associated cognitive dysfunction in rats: possible involvement of inhibiting hippocampal endoplasmic reticulum stress and synaptic dysfunction. Neurochem Res. 2021;46(3):611–23. https://doi.org/10.1007/s11064-020-03196-8.
38. Kuhns L, Kroon E, Lesscher H, Mies G, Cousijn J. Age-related differences in the effect of chronic alcohol on cognition and the brain: a systematic review. Transl Psychiatry. 2022;12(1):345. https://doi.org/10.1038/s41398-022-02100-y.
39. Tao L, Liu Z, Li X, et al. Oleanonic acid ameliorates mutant Aβ precursor protein-induced oxidative stress, autophagy deficits, ferroptosis, mitochondrial damage, and ER stress in vitro. Biochim Biophys Acta Mol Basis Dis. 2024;1870(8): 167459. https://doi.org/10.1016/j.bbadis.2024.167459.
40. Lei X, Tan G, Wang Y, et al. Mitochondrial calcium nanoregulators reverse the macrophage proinflammatory phenotype through restoring mitochondrial calcium homeostasis for the treatment of osteoarthritis. Int J Nanomedicine. 2023;18:1469–89. https://doi.org/10.2147/ijn.S402170.
41. Reggiani C, Marcucci L. Correction: A controversial issue: can mitochondria modulate cytosolic calcium and contraction of skeletal muscle fibers? J Gen Physiol. 2022;154(10). https://doi.org/10.1085/jgp.202213167090 92022c.
42. Reggiani C, Marcucci L. A controversial issue: can mitochondria modulate cytosolic calcium and contraction of skeletal muscle fibers? J Gen Physiol. 2022;154(9). https://doi.org/10.1085/jgp.202213167.
43. De Mario A, D'Angelo D, Zanotti G, Raffaello A, Mammucari C. The mitochondrial calcium uniporter complex—a play in five acts. Cell Calcium. 2023;112: 102720. https://doi.org/10.1016/j.ceca.2023.102720.
44. Balderas E, Lee SHJ, Rai NK, Mollinedo DM, Duron HE, Chaudhuri D. Mitochondrial calcium regulation of cardiac metabolism in health and disease. Physiology (Bethesda). 2024;39(5). https://doi.org/10.1152/physiol.00014.2024.
45. Popov LD. Mitochondria as intracellular signalling organelles. An update. Cell Signal. 2023;109: 110794. https://doi.org/10.1016/j.cellsig.2023.110794.
46. Li X, Zhao X, Qin Z, Li J, Sun B, Liu L. Regulation of calcium homeostasis in endoplasmic reticulum-mitochondria crosstalk: implications for skeletal muscle atrophy. Cell Commun Signal. 2025;23(1):17. https://doi.org/10.1186/s12964-024-02014-w.
47. Walkon LL, Strubbe-Rivera JO, Bazil JN. Calcium overload and mitochondrial metabolism. Biomolecules. 2022;12(12). https://doi.org/10.3390/biom12121891.
48. Bertero E, Popoiu TA, Maack C. Mitochondrial calcium in cardiac ischemia/reperfusion injury and cardioprotection. Basic Res Cardiol. 2024;119(4):569–85. https://doi.org/10.1007/s00395-024-01060-2.
49. Tufvesson-Alm M, Shevchouk OT, Jerlhag E. Insight into the role of the gut-brain axis in alcohol-related responses: Emphasis on GLP-1, amylin, and ghrelin. Front Psychiatry. 2022;13:1092828. https://doi.org/10.3389/fpsyt.2022.1092828.
50. Tsermpini EE, Plemenitaš Ilješ A, Dolžan V. Alcohol-induced oxidative stress and the role of antioxidants in alcohol use disorder: a systematic review. Antioxidants (Basel). 2022;11(7). https://doi.org/10.3390/antiox11071374.
51. Zhou Z, Bai Y, Gu X, et al. Membrane associated RNA-containing vesicles regulate cortical astrocytic microdomain calcium transients in awake ischemic stroke mice. Adv Sci (Weinh). 2024;11(46): e2404391. https://doi.org/10.1002/advs.202404391.

Publisher's Note